Construction of a Practical Hyperspectral Image Acquisition System

R. J. Bowmaker, R. J. Dunn, K. B. Moynihan, T. J. Roper, M. Andrews

Department of Electrical & Computer Engineering, University of Auckland, New Zealand.

Abstract—A hyperspectral image acquisition system has been constructed to collect data in the visible and near-infrared wavelength bands and to support research in imaging spectroscopy. The design solves a number of practical difficulties associated with hyperspectral imaging related to workflow, exposure budget, reflectance calibration and, most importantly, chromatic aberration. Chromatic aberration, present in nearly all non-monochromatic images, is particularly severe in hyperspectral images and has been significantly reduced by tracking the focal length of the lens as the wavelength changes. Attendant problems such as lens growth during focussing have also been addressed. The system is tightly integrated with software and streamlines an otherwise laborious and potentially error-prone capture process. The system is shown to provide higher quality images (as measured by the modulation transfer function) in an efficient manner with minimal chromatic aberration, simplified workflow and efficient exposure times.

I. Introduction

Conventional trichromatic imaging systems, such as consumer-grade digital cameras, portray the colours apparent in a scene with sufficient accuracy for a human observer. These qualitative systems are designed to approximate the spectral sensitivity of the human visual system; additional spectral information that cannot be perceived by humans is considered superfluous and not recorded. However, when these cameras are used for quantitative image processing, the spectral content in these images is actually very poor and techniques that require spectral information must make do with qualitative data at best.

Hyperspectral imaging goes beyond the qualitative trichromatic approach by capturing and combining monochromatic images at a large number of wavelength bands, typically spanning the visible and infra-red spectra [1]. Using such fine spectral resolution provides a unique view of a scene that is not otherwise available. The instrument that collects hyperspectral images is called an *imaging spectrometer*, since each pixel in the image has an associated spectrum, the data is commonly formatted in a three-dimensional structure known as a data cube [2].

Light reflected from the surface of an object results from the interaction of incident photons with the surface atoms of the object, and thus contains important information about the surface properties of the object. Processing is required to determine the reflectance function of the surface (a property intrinsic to the material and independent of the light source) from which various inferences can be made. For example, in remote sensing it is frequently possible to identify material compositions from careful analysis of the reflectance. Hyperspectral images provide access to these unique spectral data in a way not possible with standard trichromatic images [1].

The use of imaging spectrometers has been dominated by remote sensing, the field for which it was developed [3]. However, the quantity of data and the array of analytical techniques with which to extract useful information make hyperspectral imaging suitable for many applications outside this field [4], [5].

Nevertheless, this technology has only recently been adopted outside the remote sensing community, due largely to the high capital costs, difficulty of image acquisition and substantial data processing requirements. Consequently, turnkey imaging spectrometers remain uncommon and expensive compared to custom-built designs; although the latter generally require more development time.

Designing a custom system has some additional benefits over purchasing a turn-key system. The performance of the device, such as spectral range, spatial and spectral resolution, system throughput, etc, can be tailored for particular applications; as requirements change over time, further parts can be acquired to produce a modular, versatile system.

The general trend is that imaging spectrometers are getting cheaper, which suggests that turn-key systems will be more common in the near future. Presently, this is not the case; the purpose of this paper is to provide a practical guide on how to design and construct a scientific-grade imaging spectrometer.

A variety of hyperspectral techniques are outlined in § II, followed by a description of the relevant prerequisites of our research (§ III). The conceptual (§ IV), hardware (§ V), and software (§ VI) design of the system is presented next. A solution to chromatic aberration, which is particularly troublesome for hyperspectral imaging, is also presented. The remaining sections discuss various design decisions (§ VIII), and demonstrate the performance of the camera (§ VII).

II. Hyperspectral techniques

The primary challenge of hyperspectral image capture arises from its three-dimensional nature. While two-dimensional trichromatic images can be captured at once using a 2D Bayer-filtered CCD (Charge-Coupled Device) array, the third (spectral) dimension makes it impractical to capture the entire image simultaneously. Since current imaging sensors are constrained to just two dimensions, a third dimension (either spatial or spectral) must be synthesised over time.

Hyperspectral line scanners form an image of only one line in the scene [1]. This linear image is then dispersed using a prism or diffraction grating, to form an image which is spatial in one dimension and spectral in the other. A complete hyperspectral image is formed by scanning over the second spatial dimension. Line scanners are predominant amongst aerial and spacecraft remote sensing, since the subject of the image is rigid and stationary, and the spatial scanning motion is conveniently provided by the motion of the aircraft or spacecraft [1].

An alternative approach makes use of a tuneable optical filter, which acts as a narrow band-pass filter [6]. A monochromatic camera takes an image through the optical filter, forming an image at the wavelength selected by the filter. The filter's bandpass range is then stepped (tuned) through the wavelengths of interest, and an image taken at each wavelength.

The tuneable filter can be incorporated to the imaging system either on the subject side of the lens, or on the imaging sensor side. One could also allow the filter to be included in the middle of the lens, but such an approach would require a non-standard, expensive lens designed specifically for this purpose.

Placing the filter on the subject side of the lens is akin to placing a tube on the end of the lens, causing image vignetting unless the focal length of the lens is large. This is because the filter is optically thick and has an aperture with a small diameter, making the use of wide-angle lenses impractical in this configuration.

Conversely, placing the filter between the lens and sensor requires relay lenses, which limit the effective numerical aperture of the primary lens, as well as compromising image quality. Relay lenses are required because a lens is designed to form an image at a specified distance behind the lens, as specified by the lens mount's *flange focal distance*. Adding a filter between the lens and camera increases the separation distance between the two, so relay lenses are needed to direct the light through the filter and re-form the image on the camera sensor.

As compared to traditional monochromatic and trichromatic imaging, the amount of light reaching the camera's sensor is greatly attenuated by the tuneable filter, which rejects wavelengths outside the very narrow ($\sim 10\,\text{nm}$ FWHM[1]) passband. This is further compounded by attenuation even within the passband, which is especially severe when the filter is tuned to wavelengths at either end of its range. Long exposure times are therefore required, an issue which is revisited in § VI.

III. OUR DESIGN

The camera design is tailored to the varied requirements of our research programme. This involves hyperspectral data acquisition of animate subjects (e.g. humans), inanimate biological matter (e.g. fruit) and forensic objects and locations

---

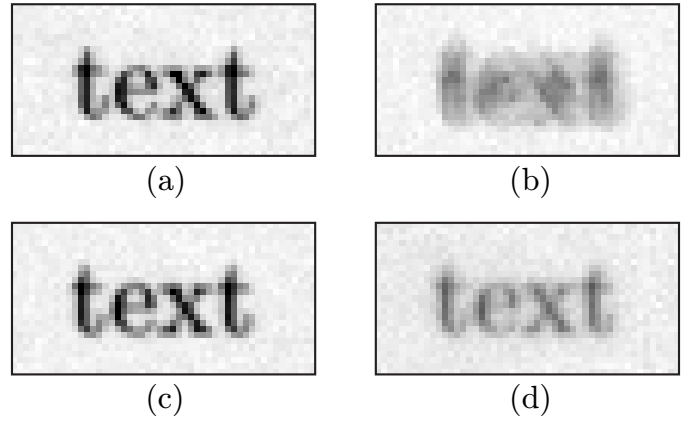[1]The full-width half-maximum (FWHM) is one common metric used to quantify filter bandwidth.

Fig. 1. Chromatic aberration from an 'achromatic' lens. (a) Focused text at 680 nm. (b) The same text imaged at 550 nm, displaying defocus aggravated by spherical aberration. (c) Same image as b, except refocused. (d) A broadband image of the same target, displaying reasonable focus and decreased contrast.

(e.g. crime scenes). From this list, human subjects are the most challenging to image as they are averse to bright light, which increases required exposure times, and their general inability to remain perfectly still can cause problems with a lack of spatial registration between frames.

Line scanners can be used in terrestrial applications, where a mirror galvanometer is used to provide the spatial scanning action. However, line scanners are not suitable for animate subjects, since any movement during exposure will distort the final image. Without elaborate precautions, this distortion is unknown and uncorrectable, so a line scanning system was not explored further.

We incorporated a tuneable optical filter, because each frame is known to be spatially self-consistent, so subject movement is more easily detected and corrected. Specifically, an LCTF (Liquid Crystal Tuneable Filter) was used [7]. Relay lenses were ruled out as the reduction in effective primary lens aperture potentially leads to increased sensor exposure time and motion blur. Thus, placing the filter on the subject side of the lens was chosen because the restriction to large focal lengths would not impact our current research projects.

IV. DESIGN DETAILS

Digital cameras and tuneable filters can capture images over a limited range of wavelengths. To expand this range, we constructed a system comprising two sets of cameras, lens, tuneable filters, and associated mounting hardware. The cameras are positioned with a minimal distance between them, to reduce the parallax error between images from the two cameras.

Axial chromatic aberration is a variation of the focal length of a lens due to the inevitable variation (dispersion) of a glass's refractive index with respect to wavelength. Lens designers can create an *achromatic* lens by combining lens elements with differing refractive properties to form a compound lens. An achromatic lens features much reduced aberration, and unlike a simple lens, certain pairs of wavelengths focus at precisely the same distance from the lens. However, all other wavelengths
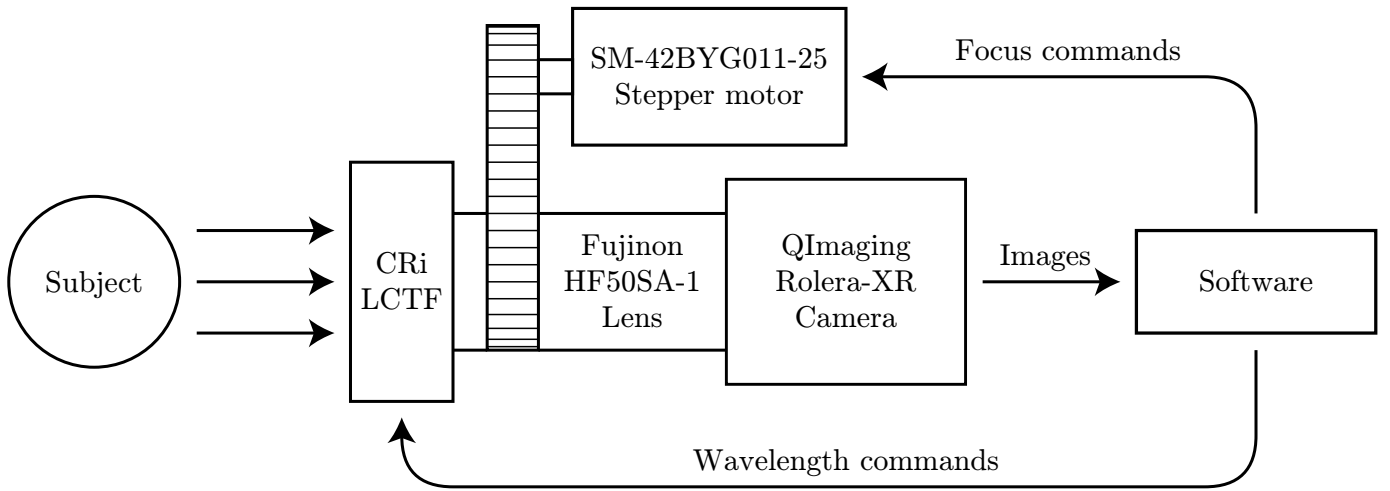
Fig. 2. The hyperspectral camera system. Light reflected from the subject is filtered by the LCTF before being captured by the lens and camera. Software then processes these images, adjusting the filter's bandpass wavelength to sweep through the wavelengths of interest. The software controls focus via the stepper motor.

still focus at different distances from the lens, so the chromatic aberration is only reduced, not eliminated [8].

While *apochromatic* and *superachromatic* lenses extend the number of simultaneously corrected wavelengths to three and four respectively, no combination of a finite number of glass types known today can compose a lens which is perfectly achromatic across a continuum of wavelengths [8]. Thus, it is practically impossible to construct a lens which is completely free of chromatic aberration. *Reflex* (mirror-based) lenses exist and are immune to chromatic aberration because they rely of reflection rather than refraction, but are often specifically designed for microscopy or telescopy.

Chromatic aberration is particularly problematic for hyperspectral imaging. At any given focus setting, achromatic lenses focus some wavelengths of light correctly, while others are significantly out of focus. A standard colour camera integrates over a wide range of wavelengths, combining both focused and unfocussed light. This is perceived as a relatively sharp image with a loss of contrast due to the unfocussed light (Figure 1d). Hyperspectral cameras, on the other hand, record all wavelengths individually, and so the poorly focused wavelengths form unacceptable images (Figure 1b).

Chromatic aberration can be corrected for by refocusing the lens for each wavelength, to compensate for focal length variations (Figure 1c). However, scientific and industrial lenses tend not to feature an integrated autofocus motor. Thus a stepper motor was used to drive a belt connected to the lens's focus ring to control focus.

In order to prevent the stepper motor from damaging/unseating the lens by applying excessive torque, a means of sensing the end of the focus range of the lens was required.

A torque measurement system was designed to prevent the stepper motor from damaging lenses, and to provide an automated way of determining the limits of the lens's focal range. A stalled or heavily loaded motor draws more current than a lightly loaded motor due to a reduction in back EMF (electromotive force) [9]. This can be used to detect the degree of resistance to movement seen by the motor. However, the movement of a stepper motor (and therefore, back EMF) consists of brief pulses of rapid movement followed by relatively long stationary periods [10]. Thus, a time-averaged measure of current is not a useful indicator of the torque produced. When each step is initiated the current through the stepper motor will be high, as the motor is stationary, so EMF is zero and current is maximised. As the rotor moves to the next step, there is a temporary decrease in current. The time it takes this current to settle to the holding current is indicative of the amount of energy required to complete the step. These variations are complicated by the inductive response of the motor coils. Nevertheless, torque measurement was successfully implemented by integrating holding current over the duration of each step.

Many lens barrels grow or shrink in length as they are refocused. This is problematic as tuneable filters are heavy, so cantilevering the filter from the end of the lens could lead to lens damage. The filter must therefore be fixed in place, but this would prevent the lens from changing in length if it were directly attached to the filter. The movement of the lens thus needed to be decoupled from the filter by constructing a variable-length, light-tight shroud. A design consisting of two sliding cylindrical adaptors was chosen. This allows the lens adaptor to slide within the filter adaptor, while maintaining a light-tight seal.

V. HARDWARE DESIGN

A block diagram of the system is presented in Figure 2, and an illustration is provided in Figure 3. A Fujinon HF50SA-1 C-mount lens (A) is attached to a QImaging Rolera-XR camera (B). The camera is bolted to a support rail (C) using the camera's standard tripod thread [11], [12].

A sprocket (D) is attached to the focus ring of the lens, which in turn is driven by a stepper motor (E) via a belt. The

belt is attached to a freely rotating sprocket, tensioned using a retention plate (F). The retention plate and stepper motor are supported by (G). A CRi LCTF (H) is also bolted to the support rail [7]. The gap between the lens and LCTF is bridged by a light-tight adaptor (I).

The visible-light and near infrared systems give half-angles of view of 6.6 and 6.4 degrees respectively, which is within the LCTF's half-angle of acceptance limit of 7.5 degrees [6].

VI. Software design

Software was developed to control and coordinate the camera, LCTF and lens settings. Coordinating these parameters by hand would be time consuming and tedious; the software significantly improves the simplicity and speed of the capture process. For example, an image consisting of twenty hyperspectral bands took three minutes to collect when controlled by hand, compared to only 61 seconds when controlled by the software (including a 55 second calibration procedure.) Another benefit of software control is improved repeatability.

Determining the optimum exposure time and focus setting for a hyperspectral camera can be time consuming and error prone, especially with the long exposure times often encountered with hyperspectral imaging. The software implements both automatic exposure control and autofocus to expedite this process, and improve user workflow.

The autoexposure algorithm uses the linearity of the CCD [13] to interpolate to an appropriate exposure time for the conditions in the scene. This linearity approximation only holds true when the images are not over or underexposed. If an image is overexposed a number of pixels on the sensor are saturated, meaning that the measured intensity at those pixels is a clipped version of the actual intensity. If an image is underexposed, the full dynamic range of the sensor is not used; the SNR is therefore compromised. The tests for overexposure and underexposure are based on percentiles; an image is considered overexposed if the 95th percentile pixel value is greater than 95% of full scale. Similarly, an image is considered underexposed if the 30th percentile is below 10%.

The autoexposure procedure first acquires two test images (with different exposure times) of a calibrated reflectance target [14]. These images are used to derive a linear regression relating exposure time and measured image intensity. These images must first be checked for overexposure or underexposure to ensure the expression will be valid; if the test images fail this check, a new exposure time is selected and the test images are reacquired.

Unlike many consumer digital cameras, scientific and industrial grade imaging hardware does not provide rangefinding (phase detection) functionality. The autofocus algorithm must therefore rely on recording test images and measuring the degree of sharpness in the image. The relationship between focus setting and image sharpness is theoretically unimodal, so a ternary search is employed to find the focus position which maximises sharpness [15].

A calibration mode has been implemented which sweeps through wavelengths selected by the user, performs autofocus and autoexposure on each, and stores the focus and exposure settings for later use. This will compensate for variations in illumination spectra, LCTF transmission efficiency and imaging sensor quantum efficiency. For example, a light source which outputs a great deal of light at certain wavelengths can be compensated for by decreasing exposure time at those wavelengths. As focus positions for contiguous wavelengths will tend to be very similar, a simple focus adjustment procedure is used, which tries adjusting focus one step at a time until optimal focus is found. This is faster than performing a lengthy ternary search autofocus at each wavelength. The calibration settings can be reused for consistency across multiple sessions.

Ascertaining exposure settings in advance allows the image capture process itself to be accelerated significantly – e.g., an image sequence that takes six seconds to capture, requires an additional 55 seconds to calibrate for. Reducing the required capture time increases the comfort and stability of human subjects, improving image quality and registration while reducing motion blur. The overall throughput of the system is improved, as a single calibration step can be used for multiple subjects.

Total capture time is also reduced by operating both the visible and near infrared camera simultaneously. This decreases the time required to the maximum exposure time of the two cameras, as opposed to the sum.

VII. Results

In well-lit conditions, where exposure times are negligible, autofocus takes approximately ten seconds to complete for the visible-spectrum camera. A complete calibration sweep, which obtains exposure and focus values for every wavelength from 400 to 720 nm in 10 nm increments, takes 136 seconds. Once calibrated, only fifteen seconds are required to capture the complete set of images.

Under similar conditions, the infrared camera takes seven seconds to autofocus. A calibration sweep from 650 to 1000 nm in 10 nm increments takes approximately 120 seconds, after which a capture period of twelve seconds is required.

In order to demonstrate the improvement in image quality due to focus tracking over varying wavelengths, a test target consisting of alternating black and white bars was imaged. When the focus tracking was disabled, the camera was set to optimal focus for 550 nm. The image quality was quantified by measuring the reduction in overall contrast between the black and white bars. This metric approximates the MTF (modulation transfer function), and is plotted in Figure 4.

It can be seen that as the wavelength tends away from 550 nm, the image quality degrades as the image goes out of focus due to chromatic aberration. However, with focus tracking enabled, the image quality remains approximately equal throughout the wavelength range. The regular wave pattern that appears from 550 nm onwards is due to the constraint of the motor to quantised steps. Finer steps or a different gear ratio would eliminate the drop in quality when optimal focus lies between two motor steps.
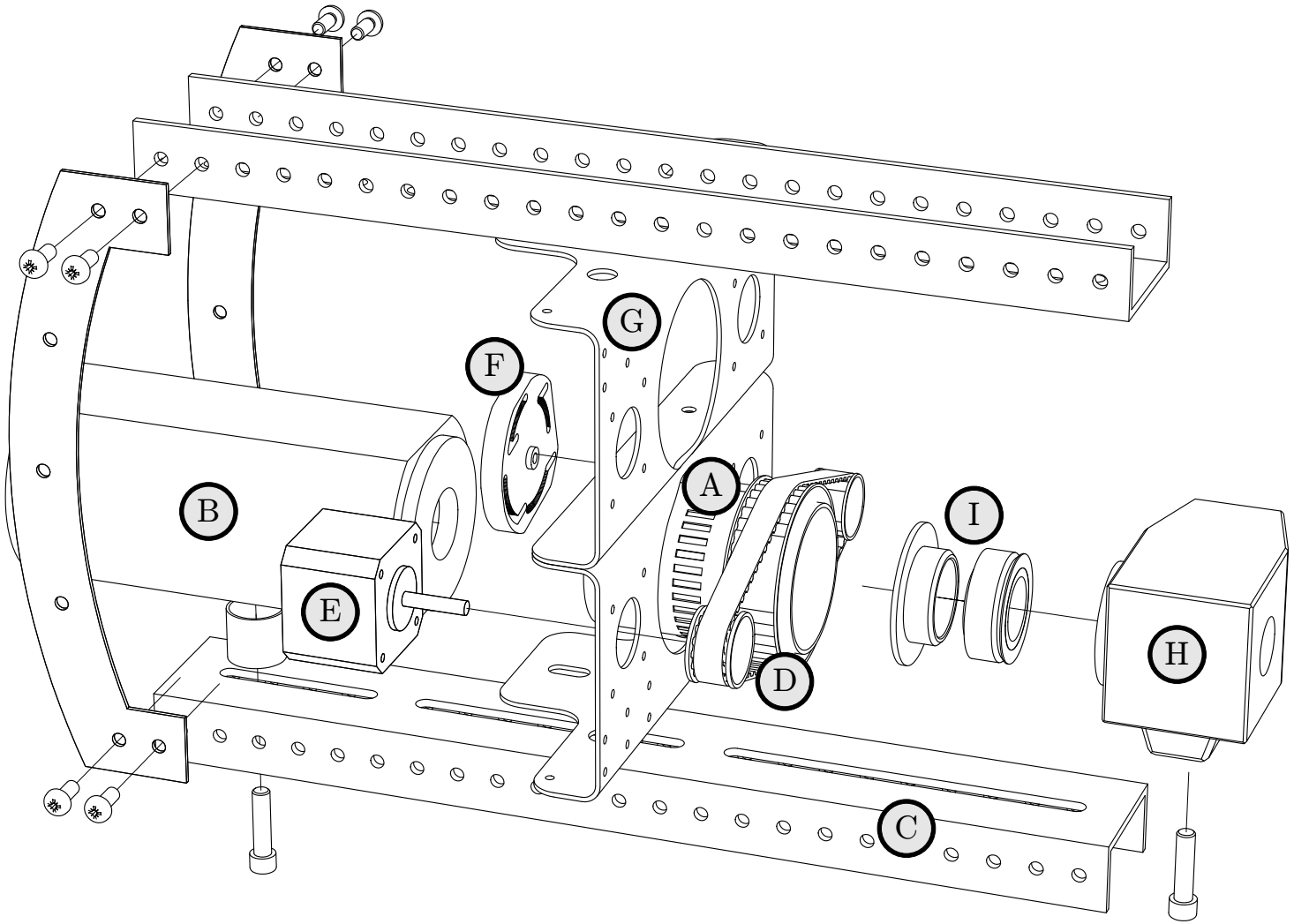
Fig. 3. The hyperspectral camera system. The upper camera is omitted for clarity.

VIII. DISCUSSION

When the system was first assembled a number of unanticipated difficulties arose. Small misalignments between the sliding adaptors connecting the lens to the LCTF added considerable friction, due to the tight clearances between the two adaptors. The extra friction exceeded the maximum torque of the motor, and there was a risk of excessive force damaging the lens or causing the adaptors to bind together. Shims were used to finely adjust the angle of the camera to reduce the misalignments and solve the friction problem.

The autofocus stepper motor would potentially sit for long periods of time drawing a large holding current ($\sim 0.5\,\mathrm{A}$). To alleviate this, there is a user-selectable option to disable the stepper motor driver after each movement. A forced minimum holding time holds the stepper in place for $100\,\mathrm{ms}$ after each sequence of steps to ensure that the lens does not move due to any elastic components of the system such as the belt. However, this does mean that the lens focus ring is free to move independently while the motor controller is unaware of any movement. In practice the torque required to do this was sufficiently large that such unreported movement is highly unlikely.

Despite the success of the autofocus system, stepper motors fundamentally only provide relative positioning. Since changes in focus are generally relative a mechanism for absolute positioning was originally not considered as a requirement. During development it was determined that long focus times necessitate the ability to remember the point of best focus for a given wavelength. The system implemented an absolute position system in software, but as it lacked true closed-loop feedback it cannot work reliably if the stepper is stalled or adjusted manually. To counter this, a servo motor or some form of reliable position feedback is recommended instead.

A free-wheeling sprocket is used to keep the belt tensioned. It is placed opposite the motor-driven sprocket, so that tension forces are symmetrical and the lens mount is not subjected to excessive bending stresses. The sprocket is held in place using a retention plate. Twisting the plate moves the axle of the sprocket toward or away from the lens, thus maintaining tension in the belt.

While a servo motor would be an ideal solution for absolute positioning and is potentially a better choice of motor, there are still benefits to a stepper motor-based system. Stepper motors provide fixed angle increments allowing discrete relative movement control. The primary problem was the lack
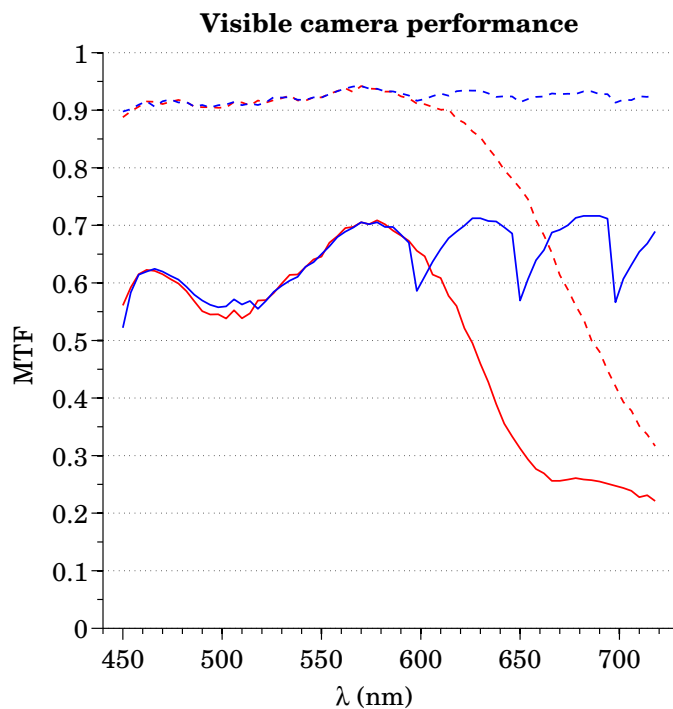
Visible camera performance

Fig. 4. Comparison of image quality with wavelength-focus adjustment (blue) and without (red). Solid lines represent modulation of fine details (30 line pairs per mm); dashed lines represent medium details (10 lp/mm).

of feedback indicating whether a step was successful. To improve this, an optical rotary encoder could be used to provide position feedback. By allowing the system to know precisely what steps have been completed, absolute positioning can be maintained while the device is powered. With a high-resolution optical encoder and a standard DC motor in place of the stepper a control system could also be used to allow for much finer control of the focus.

Although the hyperspectral system is convenient to use, re-assembling it after taking it apart is difficult as the lens and filter must be very accurately aligned to prevent excessive friction in the sliding adaptors. This friction, when left un-corrected, leads to spurious reports from the stepper motor control that the focus ring has reached the end of its travel.

Lenses are available which have a fixed external housing, where focussing occurs by moving lens elements in isolation of the surrounding structure. This would allow the adaptor to be used with no regard to precise location, or the adaptor could even be omitted altogether.

Selecting a lens based on the requirement of a fixed external housing may lead to unacceptable compromises in quality, cost, or suitability to a specific purpose. It is therefore recommended that an adaptor-based design be considered, whether it's based on sliding parts or bellows.

IX. CONCLUSION

Hyperspectral imaging is a technique which allows materials to be distinguished in situations where more conventional methods would fail to do so. However, it is inherently sus-

ceptible to chromatic aberration. A hyperspectral imaging system has been developed which incorporates autofocus and compensation for longitudinal chromatic aberration. Testing has shown that the system has practically eliminated longitu-dinal chromatic aberration. The software also automates and streamlines the capture process, resulting in a faster, more consistent, and higher quality imaging process.

REFERENCES

[1] G. A. Shaw and H.-h. K. Burke, "Spectral imaging for remote sensing," *Lincoln Laboratory Journal*, vol. 14, pp. 3–28, 2003.

[2] D. Manolakis, D. Marden, and G. A. Shaw, "Hyperspectral image pro-cessing for automatic target detection applications," *Lincoln Laboratory Journal*, vol. 14, pp. 79–116, 2003.

[3] D. Landgrebe, "Multispectral land sensing: Where from, where to?" *Geoscience and Remote Sensing, IEEE Transactions on*, vol. 43, no. 3, pp. 414–421, 2005.

[4] L. Brewer, J. Ohlhausen, P. Kotula, and J. Michael, "Forensic analysis of bioagents by x-ray and tof-sims hyperspectral imaging," *Forensic science international*, vol. 179, no. 2-3, pp. 98–106, 2008.

[5] R. Lu, "Detection of bruises on apples using near-infrared hyperspectral imaging," *Transactions of the ASAE*, vol. 46, no. 2, pp. 523–530, 2003.

[6] CRi, "VariSpec™ Liquid Crystal Tunable Filters User's Manual."

[7] Varispec filter manufacturer. [Online]. Available: http://www.cri-inc.com/

[8] M. Herzberger and N. McClure, "The design of superachromatic lenses," *Applied Optics*, vol. 2, no. 6, pp. 553–560, 1963.

[9] W. S. Wood, *Theory of electrical machines*. Butterworths Scientific Publications, 1958, p. 1.

[10] D. O'Kelly, *Performance and control of electrical machines*. McGraw-Hill, 1991, pp. 287–288.

[11] HF50SA-1 manufacturer. [Online]. Available: http://www.fujifilmusa.com/products/optical_devices/

[12] Rolera XR manufacturer. [Online]. Available: http://www.qimaging.com/

[13] D. Burt, "CCD performance limitations: theory and practice," *Nuclear Instruments and Methods in Physics Research Section A: Accelerators, Spectrometers, Detectors and Associated Equipment*, vol. 305, no. 3, pp. 564–573, 1991.

[14] Reflectance standard. [Online]. Available: http://www.labsphere.com/uploads/datasheets/diffuse-reflectance-standards-product-sheet.pdf

[15] M. Heath, *Scientific computing*. McGraw-Hill, 1997, pp. 182–184.